Electronic Supplementary Information (ESI)

Weak Pb–O of Confined [Pb–O_4] in Pyramidal Sillenite-type $Bi_{12}PbO_{20}$ for Enhanced Electrochemical Ozone Production

Huaijie Shi[a,#], Ge Feng[a,#], Suiqin Li[a], Jia Liu[a], Xinying Yang[a], Ye Li[b], Ye Lu[b], Xing Zhong[a,], Shibin Wang[a,]*, Jianguo Wang[a,]**

[a] Institute of Industrial Catalysis, College of Chemical Engineering, State Key Laboratory Breeding Base of Green-Chemical Synthesis Technology, Zhejiang University of Technology, Hangzhou, China.

[b] Department of Environmental Health, Zhejiang Provincial Center for Disease Control and Prevention, Hangzhou, China.

H. J. Shi and G. Feng contribute to this work equally

* Correspondence and requests for materials should be addressed to X. Z. (email: zhongx@zjut.edu.cn), or to S. B. W. (email: wangshibin@zjut.edu.cn), J. G. W. (email: jgw@zjut.edu.cn).

Contents

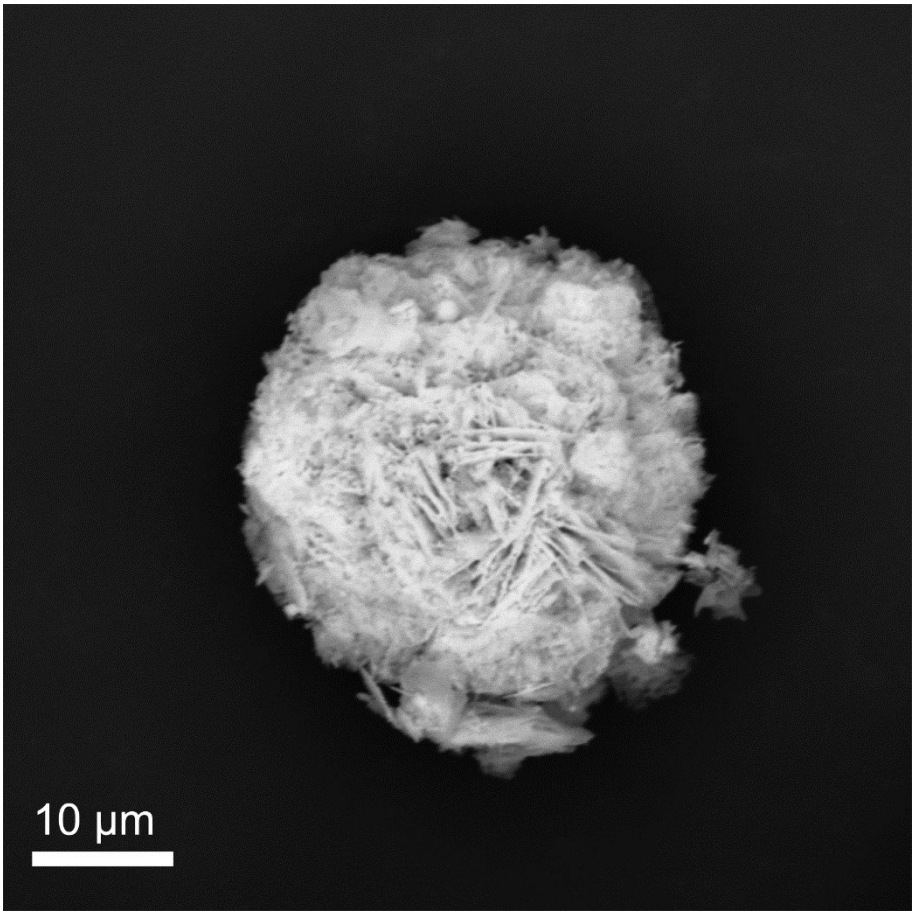

Fig. S1. SEM image of Bi_2O_3 flower.

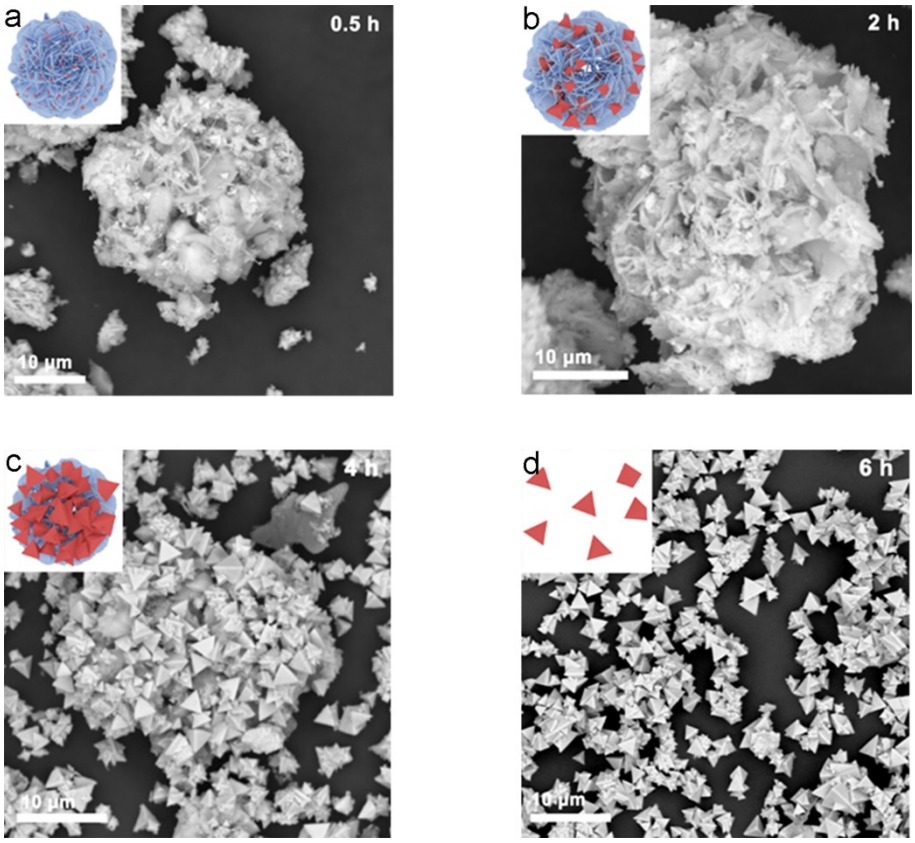

Fig. S2. SEM images of $Bi_{12}PbO_{20}$ at different reaction time. **(a)** 0.5 h; **(b)** 2 h; **(c)** 4 h; **(d)** 6 h.

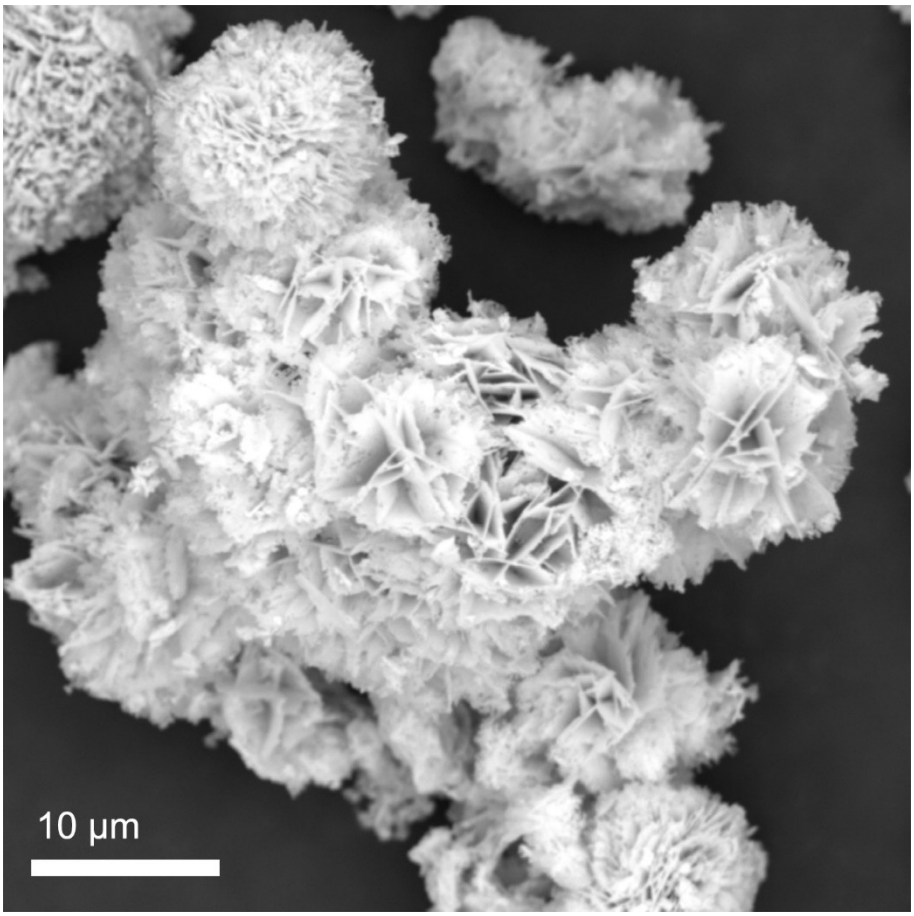

Fig. S3. SEM image of $Bi_{12}PbO_{20}$-no NaOH.

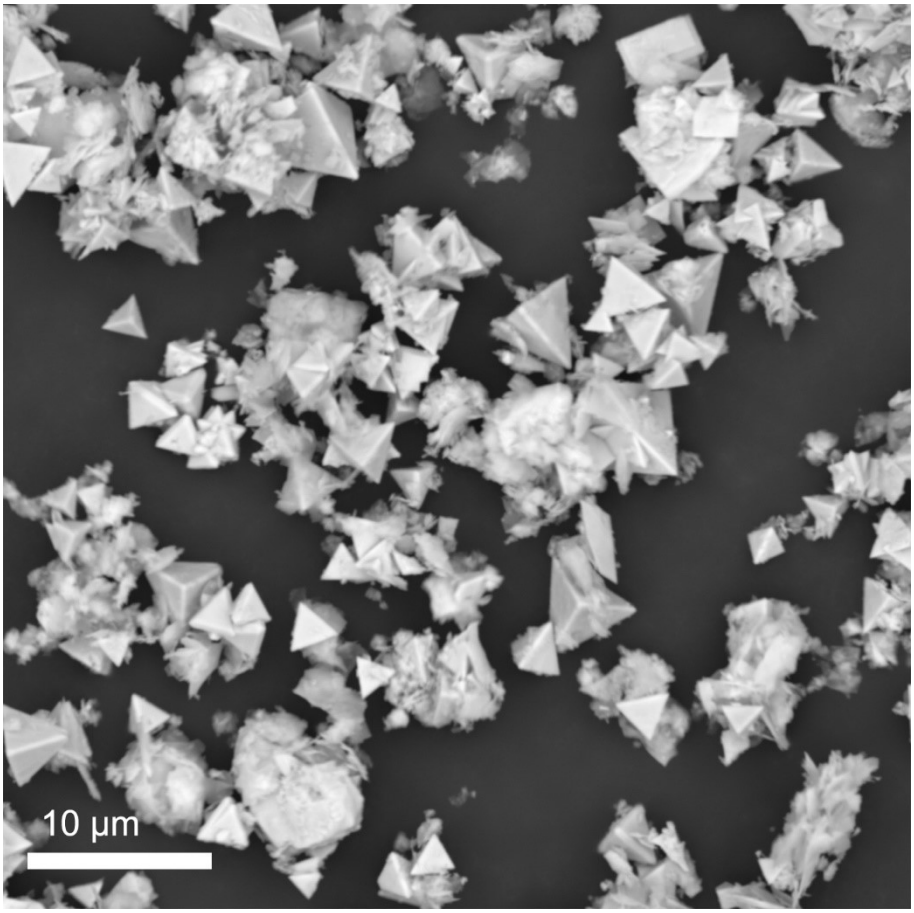

Fig. S4. SEM image of $Bi_{12}PbO_{20}$-no PVP.

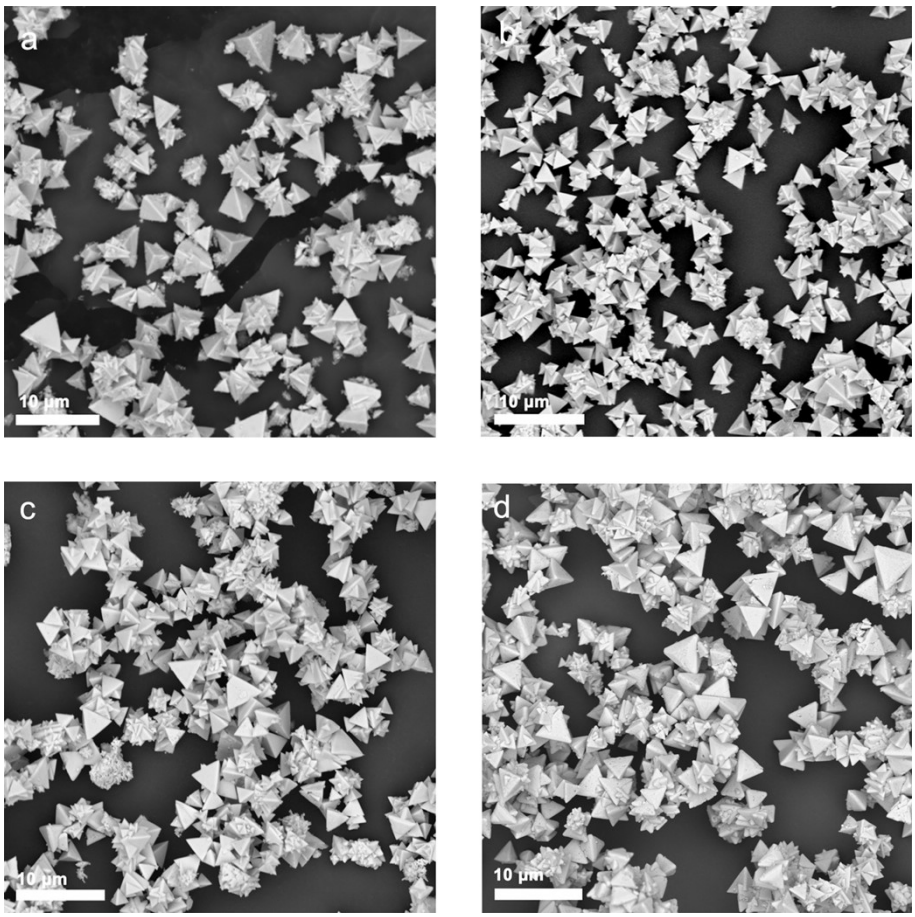

Fig. S5. SEM images of $Bi_{12}PbO_{20}$-1, 2, 4 and 5.

Table. S1. Element contents of $Bi_{12}PbO_{20}$-1, 2, 3, 4 and 5 by ICP for Bi, Pb and XPS analysis for O content (mol. %).

Samples	Pb loading (mol. %)	Bi loading (mol. %)	O loading (mol. %)
$Bi_{12}PbO_{20}$-1	0.98	37.39	61.63
$Bi_{12}PbO_{20}$-2	1.22	37.30	61.48
$Bi_{12}PbO_{20}$-3	2.00	37.08	60.92
$Bi_{12}PbO_{20}$-4	2.44	36.85	60.71
$Bi_{12}PbO_{20}$-5	3.79	36.30	59.91

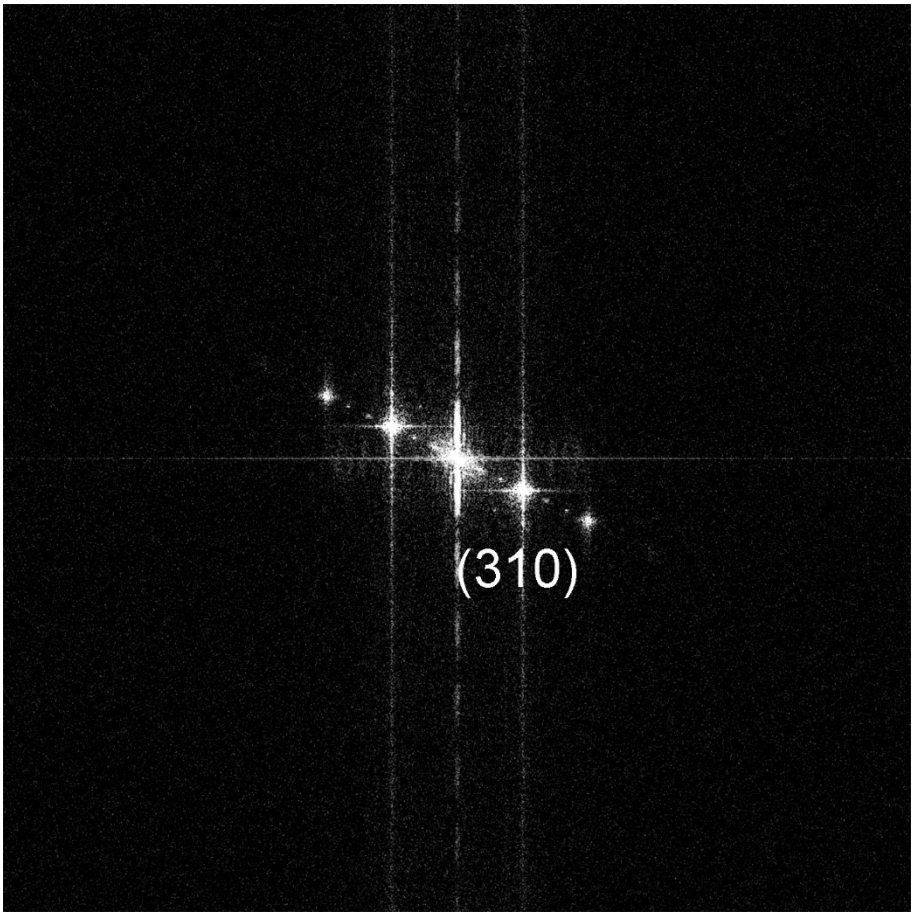

Fig. S6. The FFT pattern of $Bi_{12}PbO_{20}$-3 by STEM.

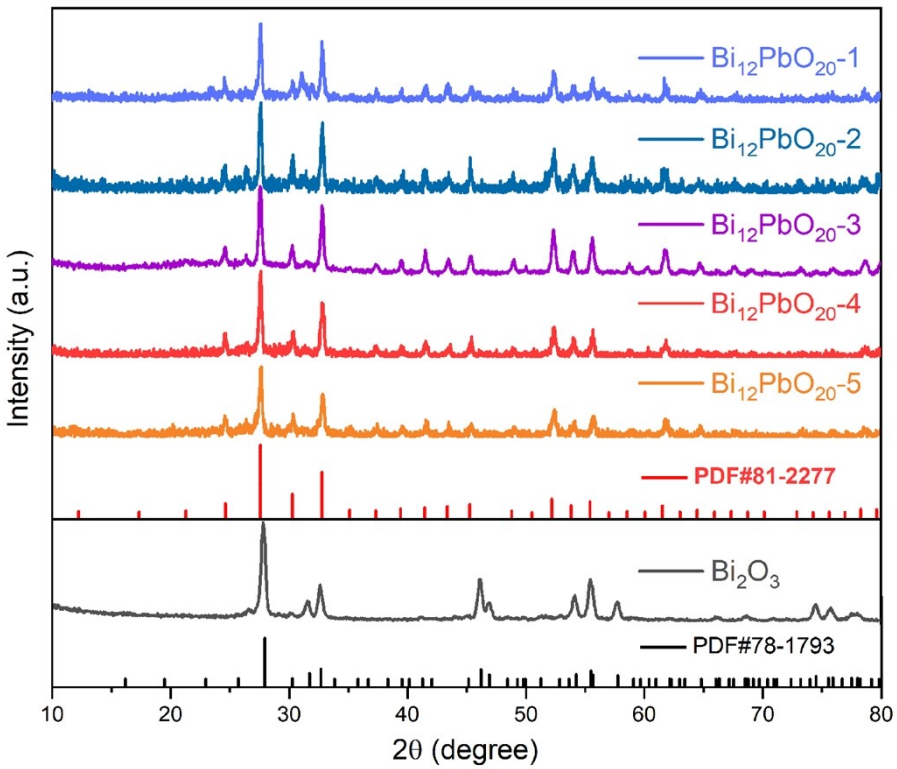

Fig. S7. XRD pattern of $Bi_{12}PbO_{20}$-1, 2, 3, 4, 5 and Bi_2O_3.

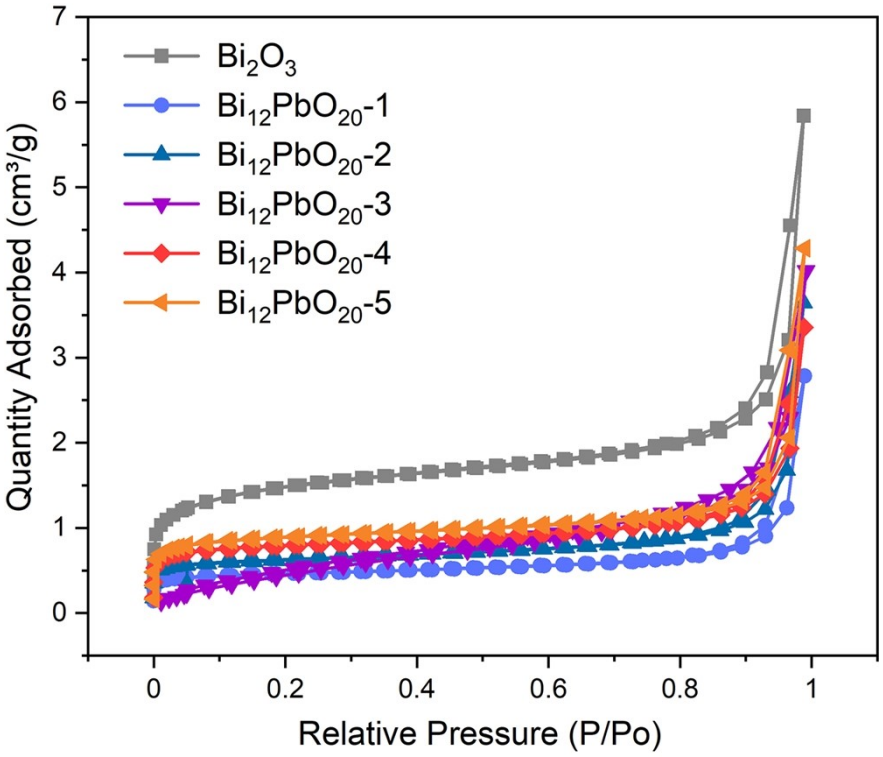

Fig. S8. N_2 adsorption-desorption isotherms of $Bi_{12}PbO_{20}$-1, 2, 3, 4, 5 and Bi_2O_3.

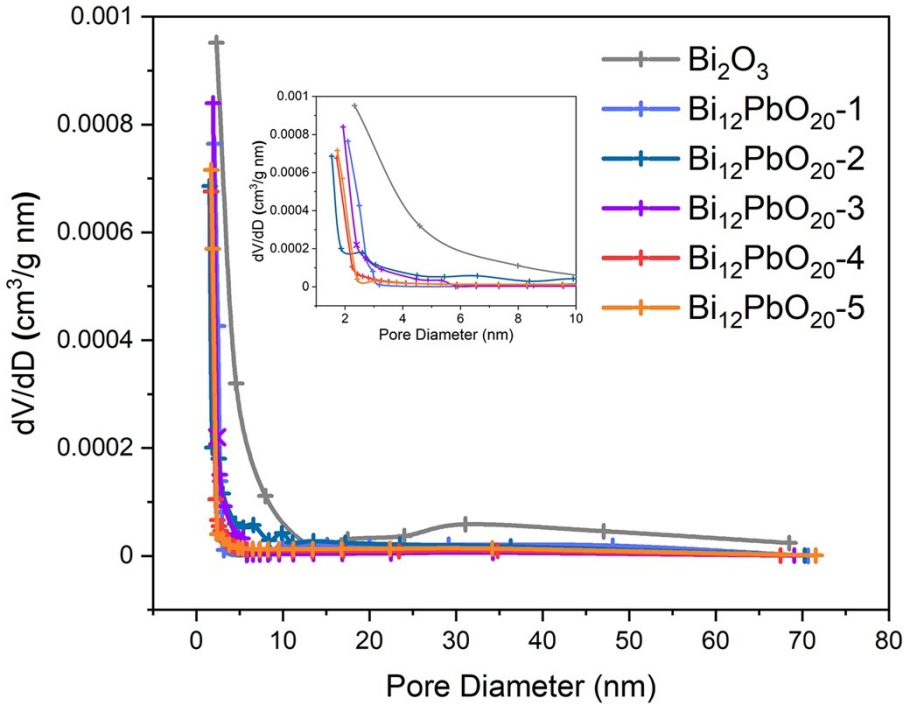

Fig. S9. The pore size distribution of $Bi_{12}PbO_{20}$-1, 2, 3, 4, 5 and Bi_2O_3.

Table. S2. Surface area and pore volume of $Bi_{12}PbO_{20}$-1, 2, 3, 4, 5 and Bi_2O_3.

Samples	Surface area (m^2 g^{-1})	Total pore Volume (cm^3 g^{-1})
Bi_2O_3	5.84	0.008180
$Bi_{12}PbO_{20}$-1	2.78	0.002434
$Bi_{12}PbO_{20}$-2	3.64	0.003936
$Bi_{12}PbO_{20}$-3	4.02	0.003094
$Bi_{12}PbO_{20}$-4	3.35	0.003651
$Bi_{12}PbO_{20}$-5	4.28	0.002934

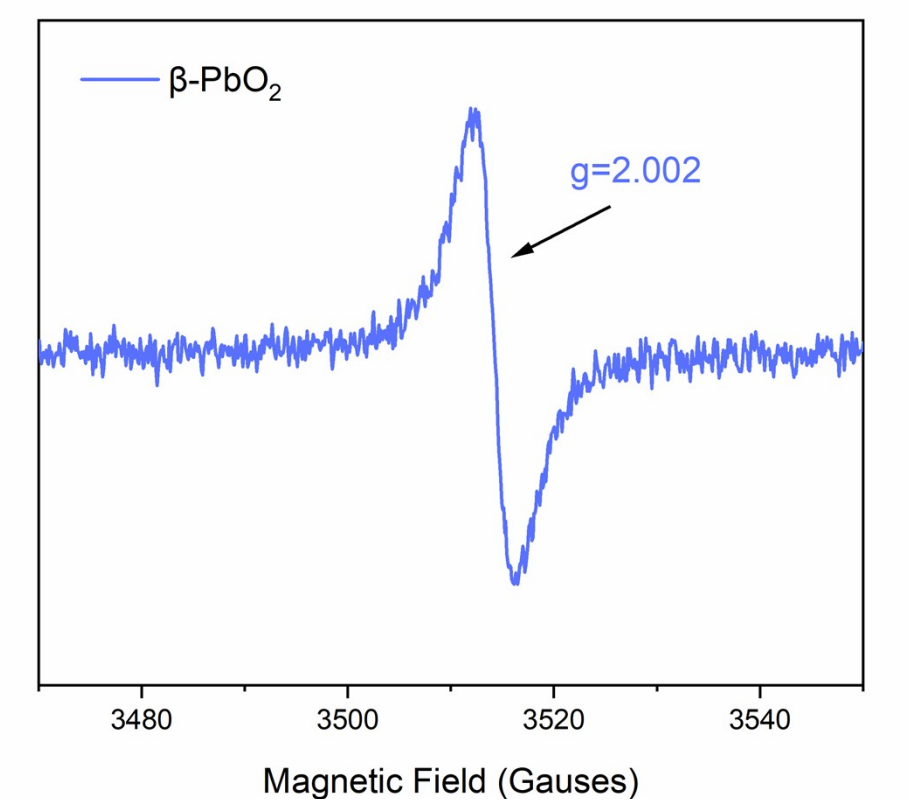

Fig. S10. Electron paramagnetic resonance test of β-PbO_2

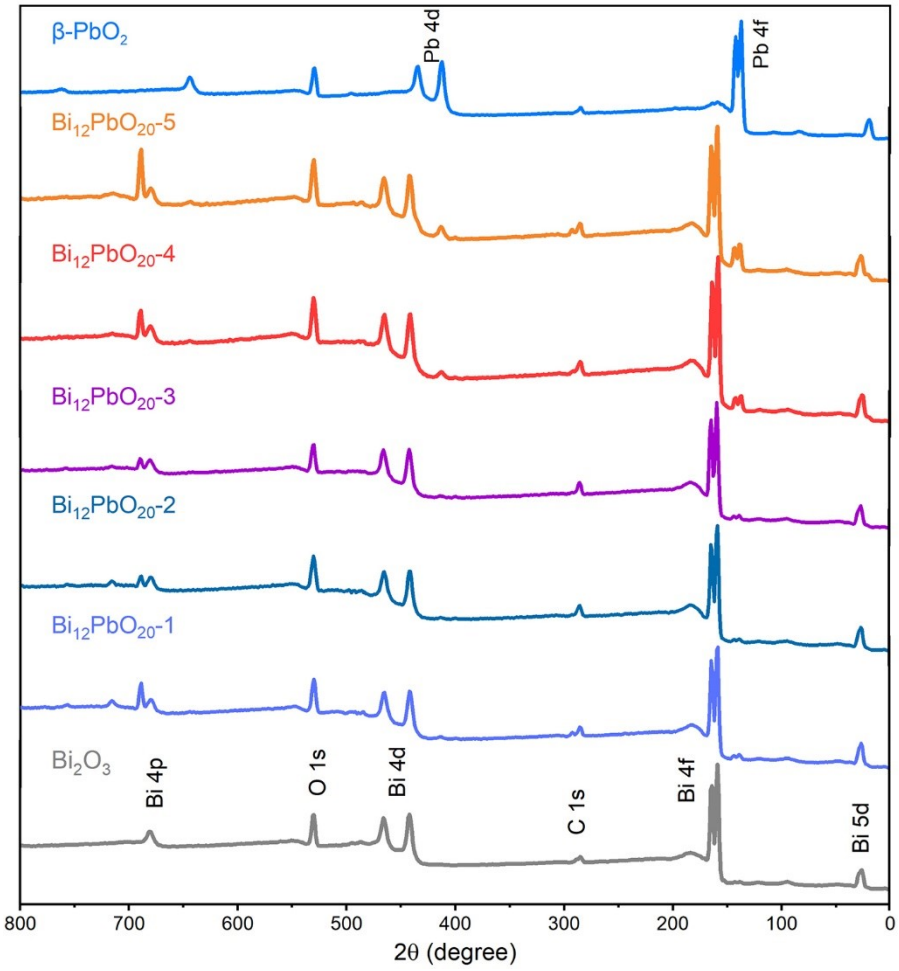

Fig. S11. XPS survey spectra of Bi_2O_3, $Bi_{12}PbO_{20}$-1, 2, 3, 4, 5 and β-PbO_2.

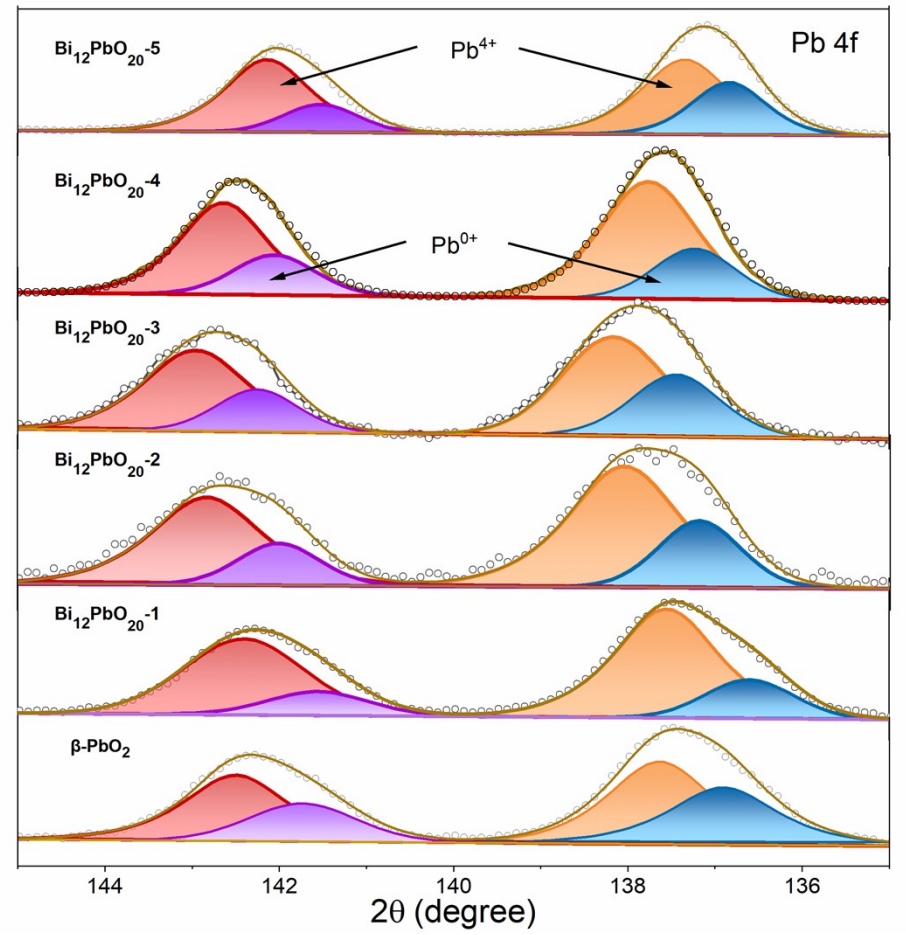

Fig. S12. High-resolution XPS spectra of Pb 4f for $Bi_{12}PbO_{20}$-1, 2, 3, 4, 5 and β-PbO_2.

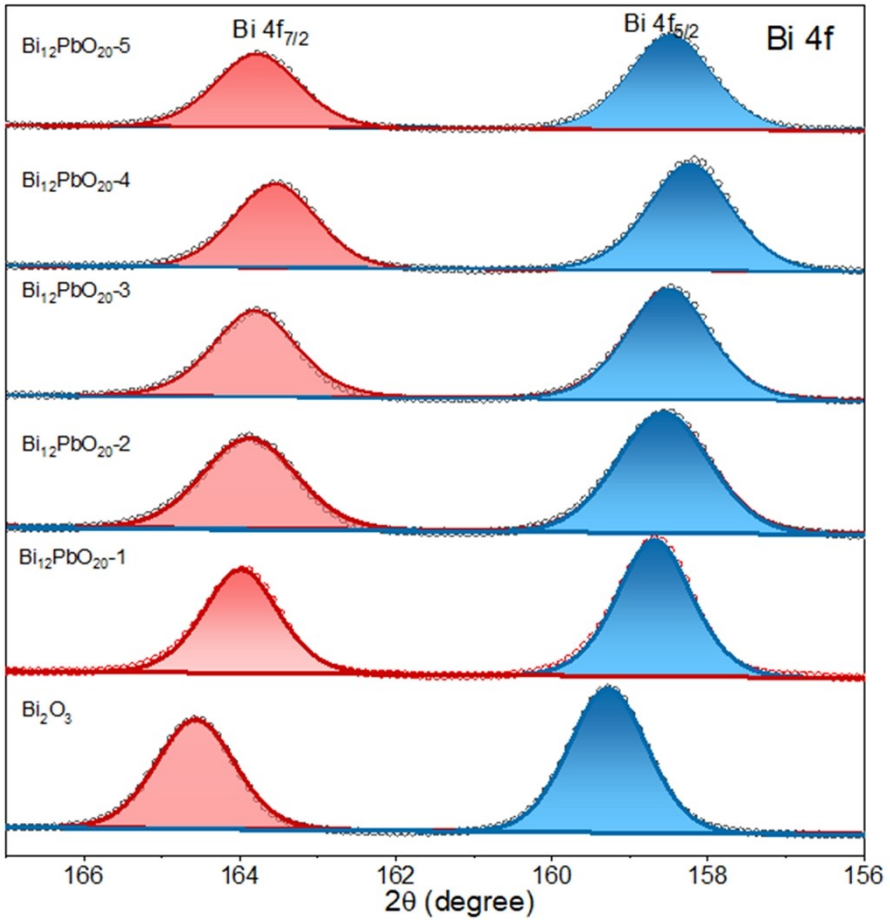

Fig. S13. High-resolution XPS spectra of Bi 4f for Bi_2O_3, $Bi_{12}PbO_{20}$-1, 2, 3, 4 and 5.

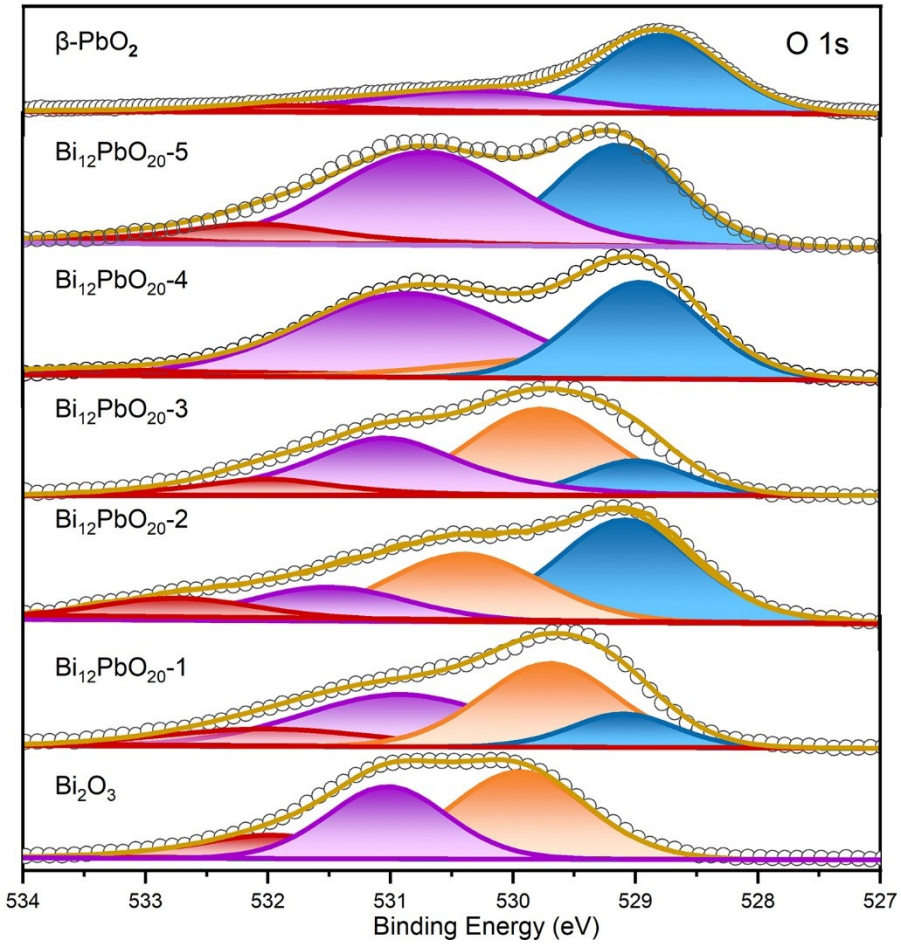

Fig. S14. High-resolution XPS spectra of O 1s for Bi_2O_3, $Bi_{12}PbO_{20}$-1, 2, 3, 4, 5 and β-PbO_2.

Table. S3. Summary of functional groups for $Bi_{12}PbO_{20}$-3 obtained from XPS analysis.

Pb 4f functional groups	Binding energy (eV)		Relative intensity (%)
Pb^{4+}	138.1	142.9	68.83
Pb^{0}	137.5	142.3	31.17
O 1s functional groups	**Binding energy (eV)**		**Relative intensity (%)**
Pb-O	529.0		12.95
Bi-O	529.8		46.90
Adsorb O	531.2		29.39
OH	532.3		10.75

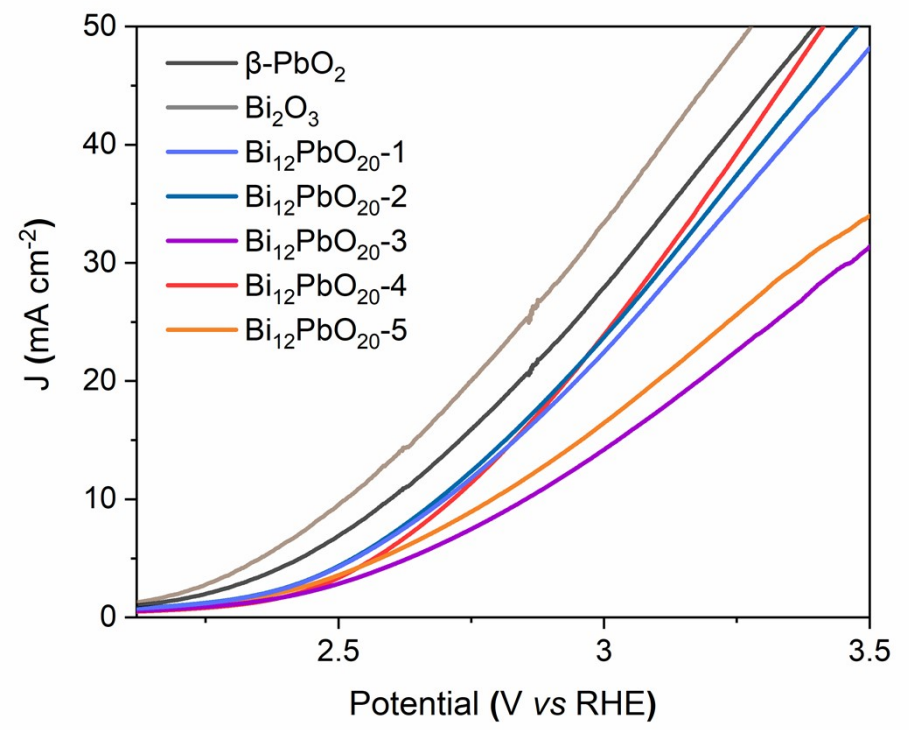

Fig. S15. Steady state polarization curves of $Bi_{12}PbO_{20}$-n (n = 1, 2, 3, 4, 5), β-PbO_2, and Bi_2O_3 after 2.12 V vs.RHE

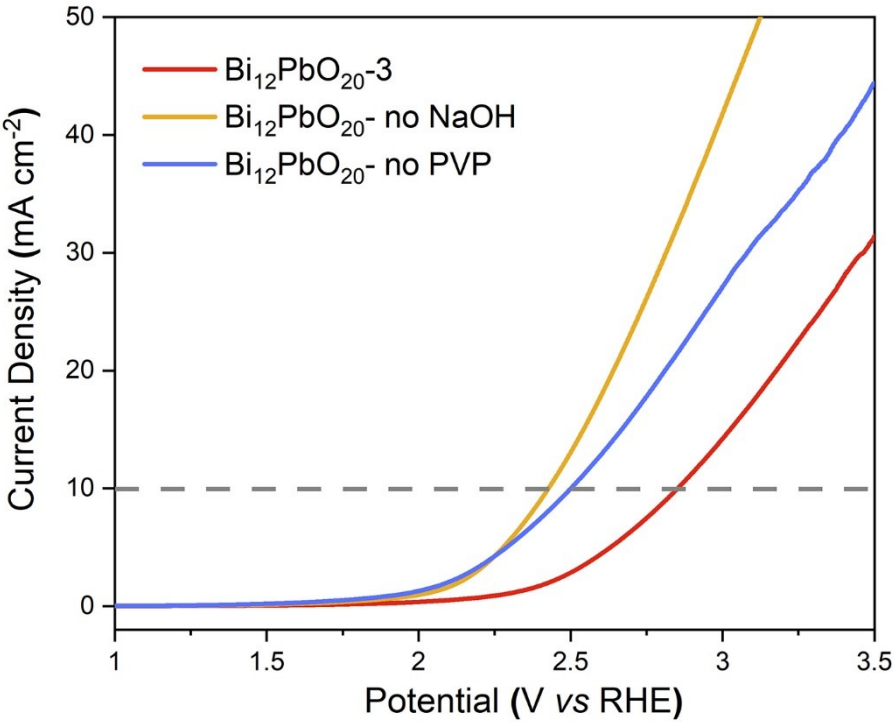

Fig. S16. Steady-state polarization curves for $Bi_{12}PbO_{20}$-3, $Bi_{12}PbO_{20}$-no NaOH and no PVP.

Table. S4. Summary of the Electrochemical Properties of prepared Electrode.

Catalysts	Tafel Slope (mV dec^{-1})	$J_{0,\ geometric}$ (mA cm^{-2})	C_{dl} (mF cm^{-2})	Relative surface area	$J_{0,\ normalized}$ (mA cm^{-2})
Bi_2O_3	548	2052	2.2	1.00	2052
$Bi_{12}PbO_{20}$-1	621	2184	5.9	2.68	780
$Bi_{12}PbO_{20}$-2	637	2172	4.6	2.09	1039
$Bi_{12}PbO_{20}$-3	667	2263	4.5	2.05	1104
$Bi_{12}PbO_{20}$-4	617	2286	3.1	1.41	1621
$Bi_{12}PbO_{20}$-5	580	2203	2.9	1.32	1669

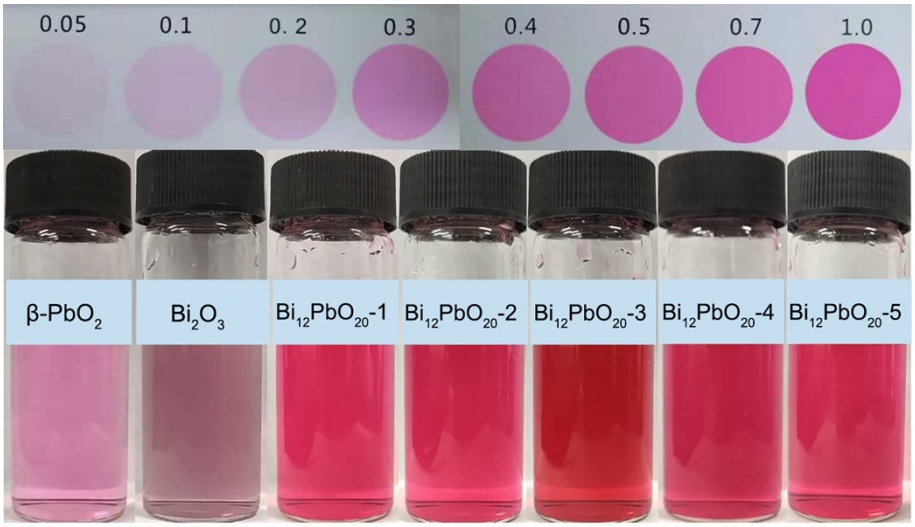

Fig. S17. Qualitative concentration test of ozone water, the color depth represents the concentration of ozone. Give a qualitative comparison on the concentration of dissolved ozone.

Table. S5. The anode voltage corresponding to different cell voltage.

Cell voltage (V)	Anode voltage (V)
1.5	1.315
2.0	1.542
2.5	1.846
3.0	2.159
3.5	2.390

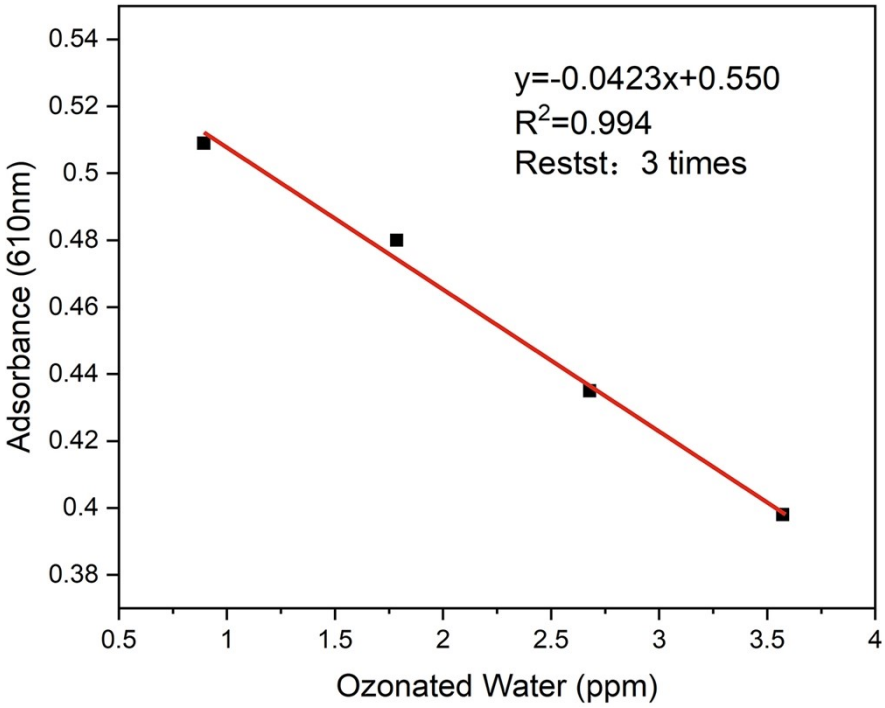

Fig. S18. The standard curve of ozonated water concentration in saturated K_2SO_4 solution.

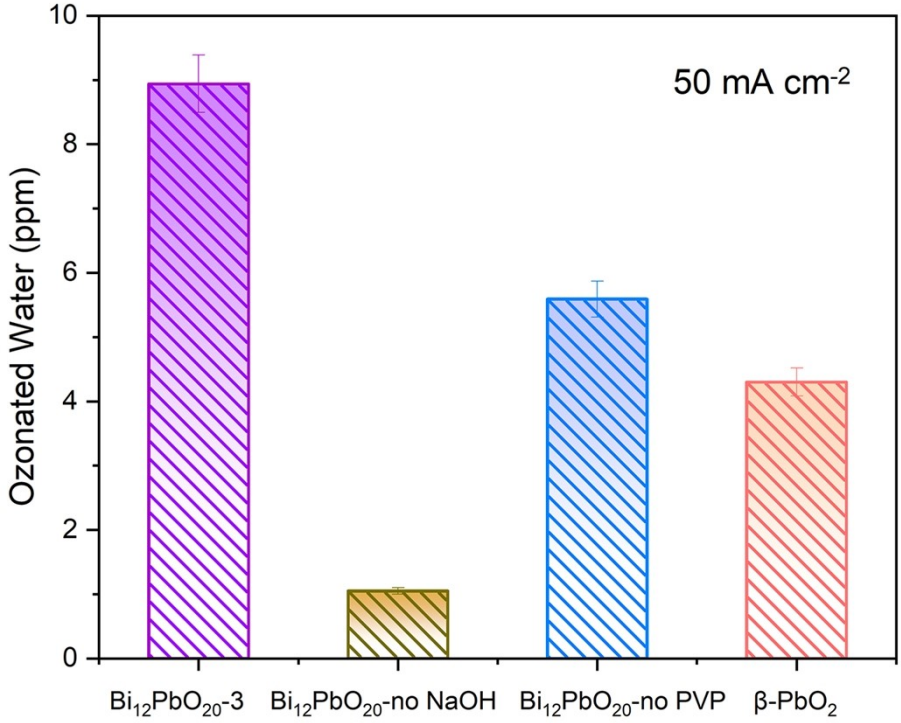

Fig. S19. Ozone Water concentrations between the $Bi_{12}PbO_{20}$-3, $Bi_{12}PbO_{20}$-no NaOH, $Bi_{12}PbO_{20}$-no PVP and β-PbO_2.

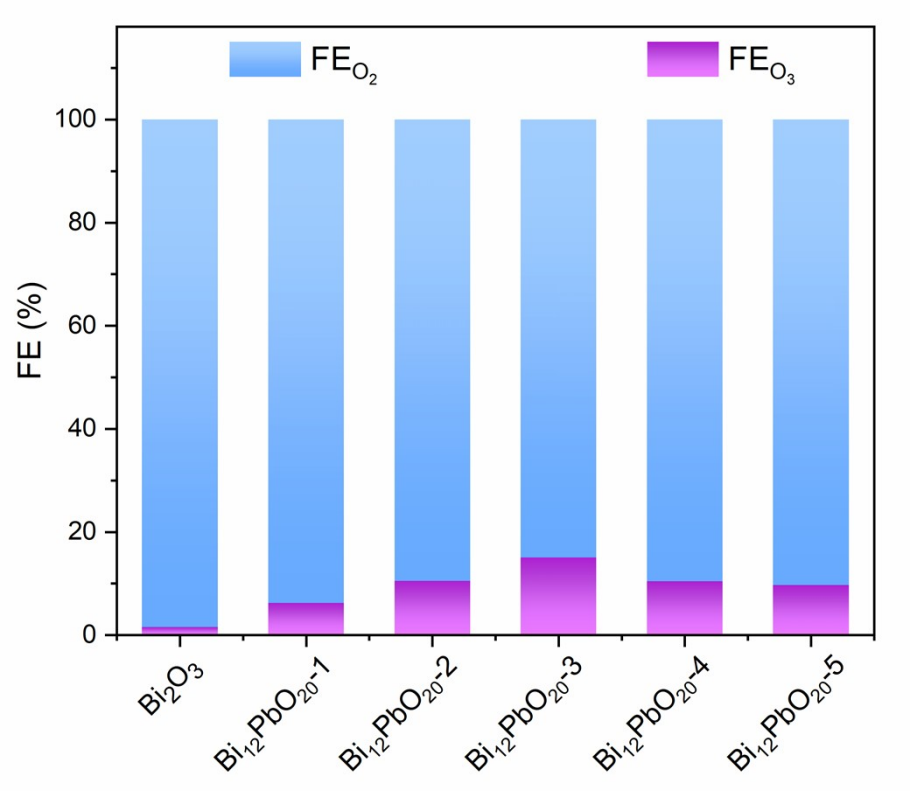

Fig. S20. The FE_{O2} of Bi_2O_3, $Bi_{12}PbO_x$-n (n=1, 2, 3, 4 and 5) at 50 mA cm^{-2}

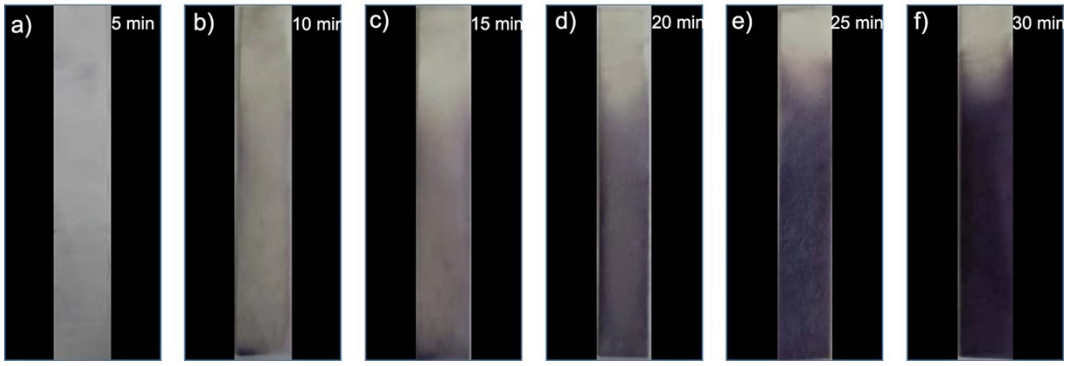

Fig. S21. Moistened starch potassium iodide paper giving a qualitative comparison on the EOP of $Bi_{12}PbO_{20}$-3 at current density of 50 mA cm^{-2}.

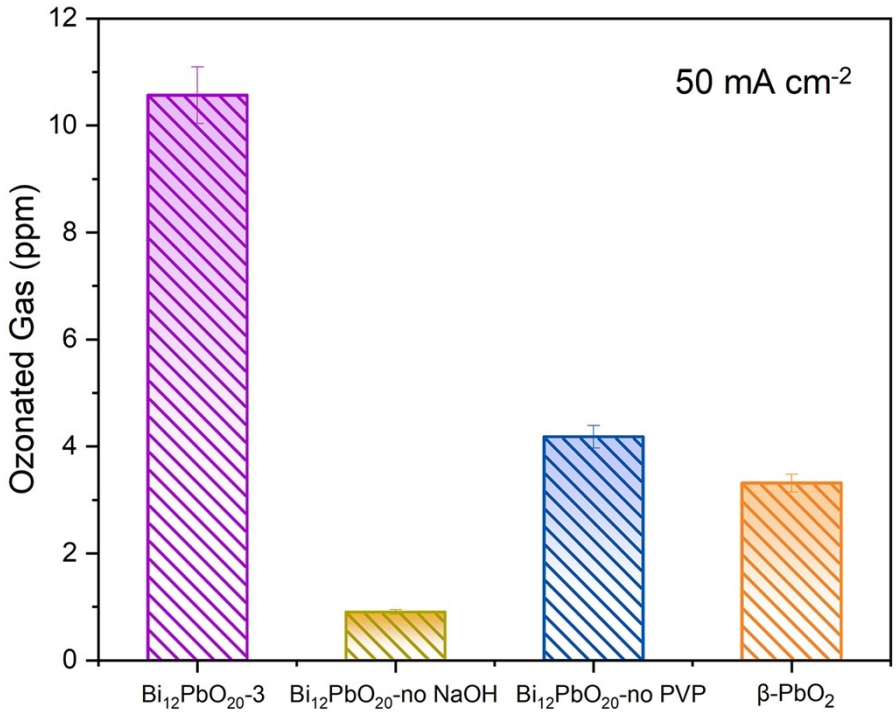

Fig. S22. Ozone Gas concentrations between the $Bi_{12}PbO_{20}$-3, $Bi_{12}PbO_{20}$-no NaOH, $Bi_{12}PbO_{20}$-no PVP and β-PbO_2.

Table. S6. The performance comparison of $Bi_{12}PbO_{20}$-3 with other electrocatalysts toward for EOP.

Catalysts	Electrolyte	Temperature	FE (%)	Ref.
$Bi_{12}PbO_{20}$-3	**Neutral media**	**25 ℃**	**15.1**	**This work**
β-PbO_2-150 NRs	Neutral media	25 °C	11.8	J. Mater. Chem. A, 9010–9017 (2021)
Pt-TaO_x/Ti	Neutral media	25 °C	11.7	*Electrochem. Commun.* ***8****, 1263-1269 (2006)*
Si/TiO_x/Pt/TiO_2	Acid medium	25 °C	9	*J. Electrochem. Soc.* ***157****, F30 (2010).*
PtZn/Zn-N-C	Neutral media	25 °C	4.2	*J. Energy Chem.* ***51****, 312-322 (2020)*
Pt-Reticulater Vitreous Carbon	Neutral media	25 °C	1.6	*J. Electrochem. Soc. 153 D207-D212 (2006)*

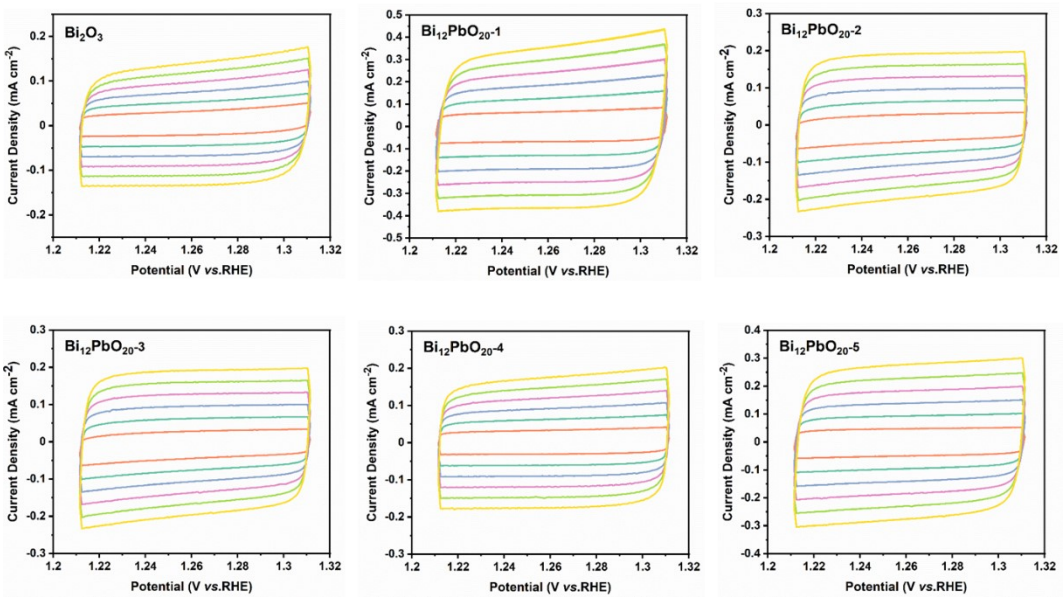

Fig. S23. CV at different scan rates in the region of 20-120 mV vs. RHE in saturated K_2SO_4 of Bi_2O_3, $Bi_{12}PbO_{20}$-1, 2, 3, 4 and 5.

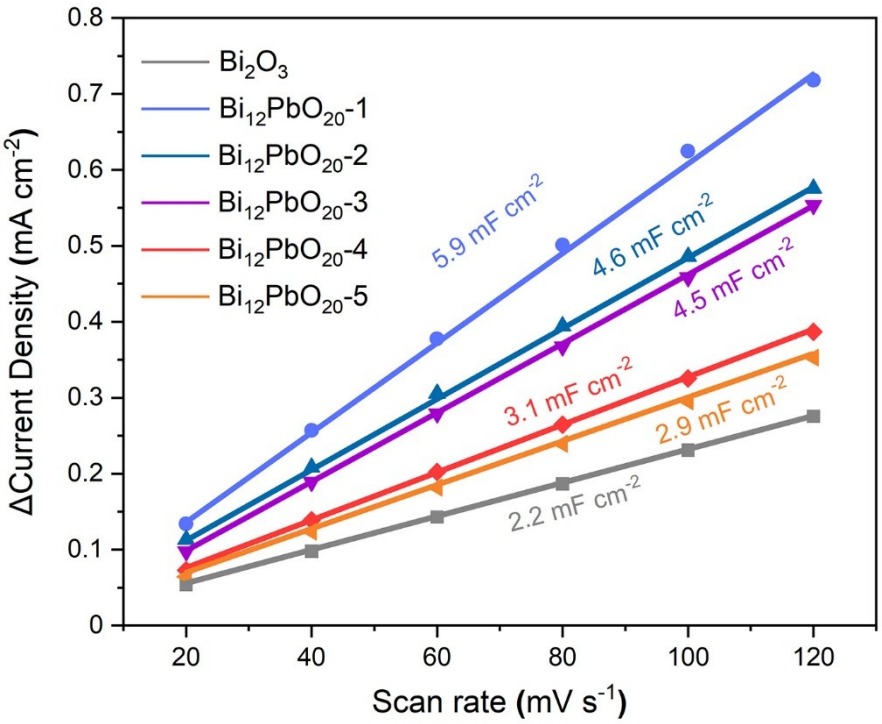

Fig. S24. Different scan rates to measure capacitive currents for Bi_2O_3, $Bi_{12}PbO_{20}$-1, 2, 3, 4 and 5.

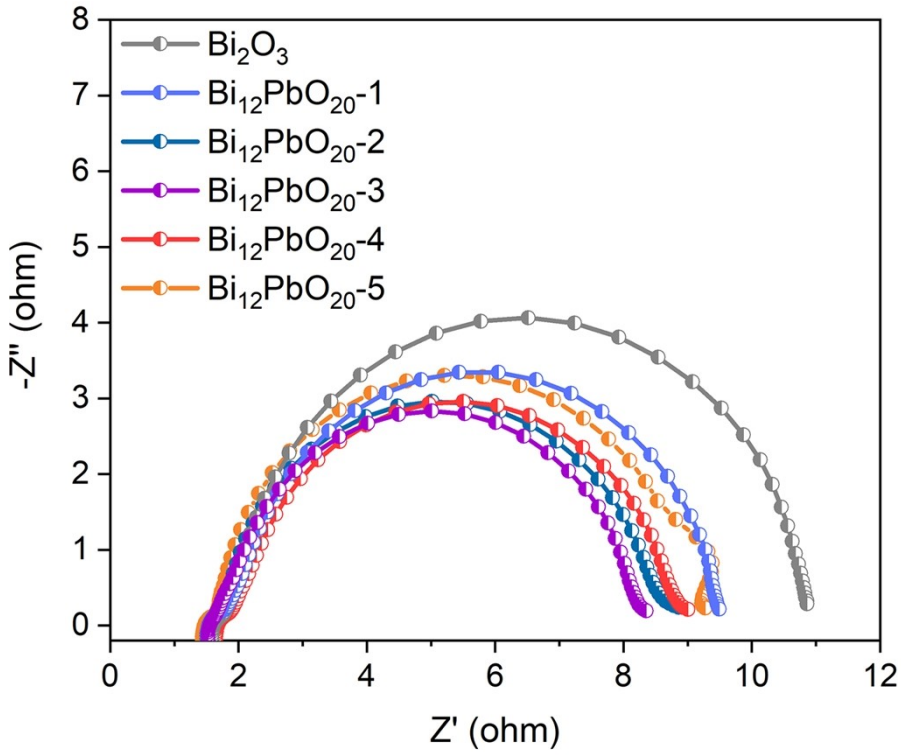

Fig. S25. Nyquist plots of Bi_2O_3, $Bi_{12}PbO_{20}$-1, 2, 3, 4 and 5.

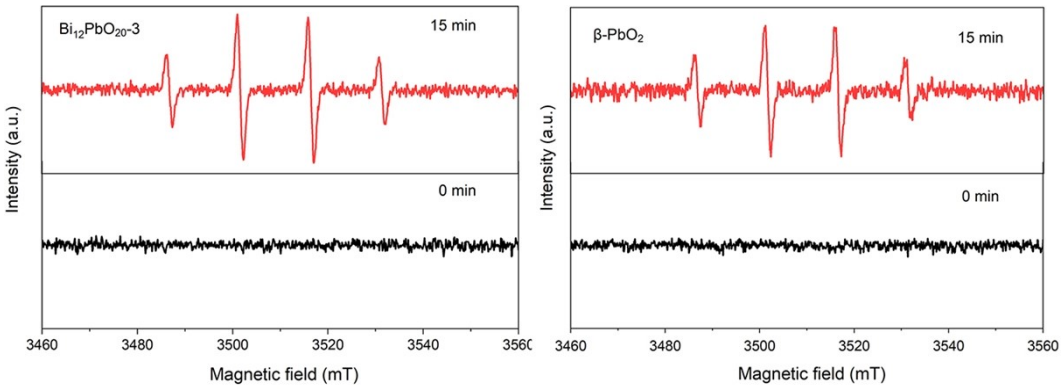

Fig. S26. ESR measurement results of DMPO-·OH for $Bi_{12}PbO_{20}$-3 and β-PbO_2.

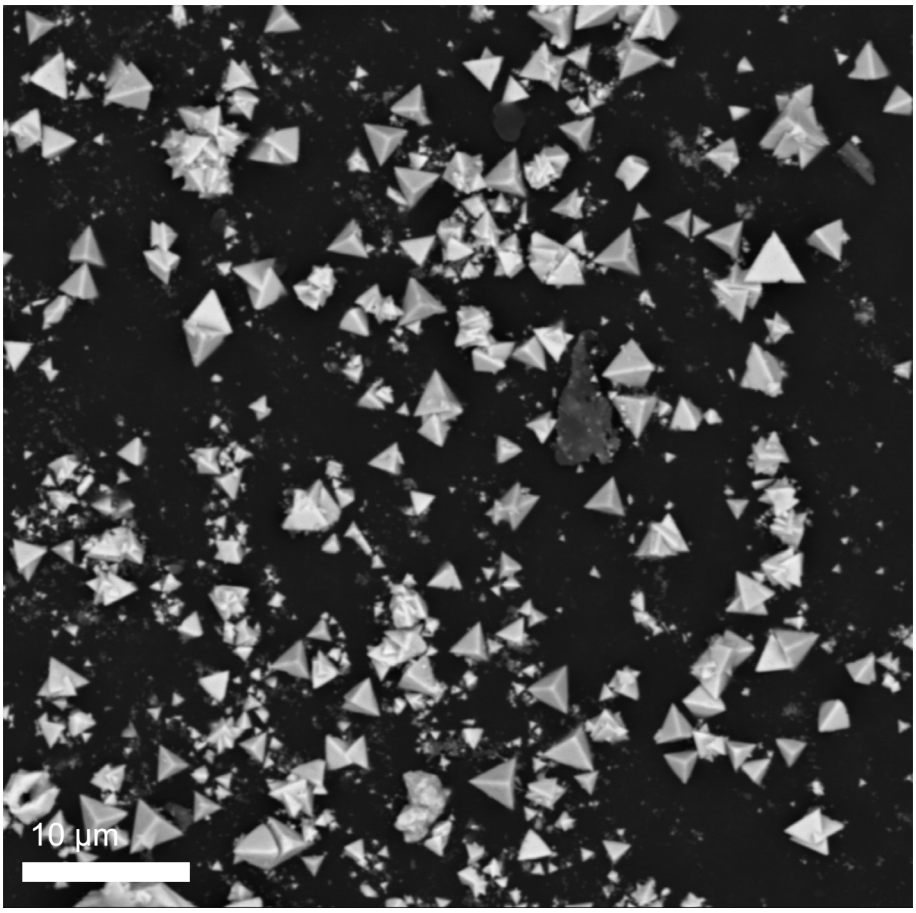

Fig. S27. SEM image of the $Bi_{12}PbO_{20}$-3 after 100 h constant potential test for EOP.

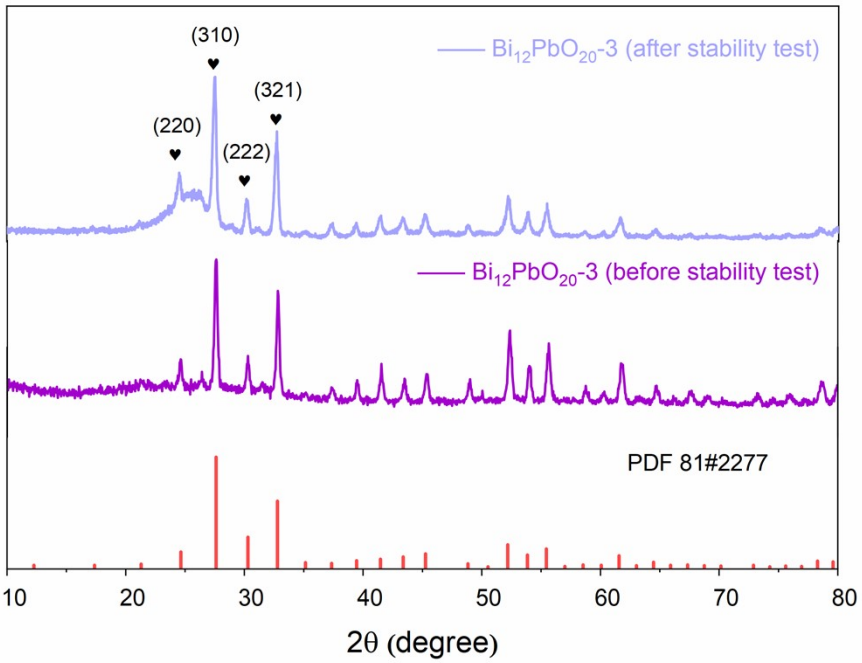

Fig. S28. XRD pattern comparison before and after stability the $Bi_{12}PbO_{20}$-3.

Table. S7. Element contents of electrolyte after the reaction by ICP for Bi and Pb

Samples	Pb (ppm)	Bi (ppm)
The electrolyte after the reaction	0.0144	0.0312

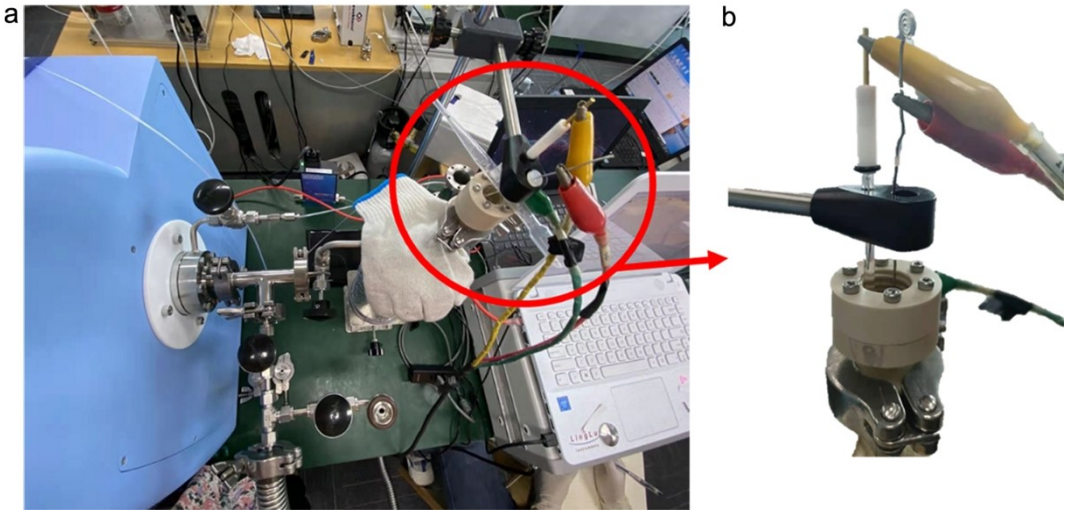

Fig. S29. (a) The photograph of the DEMS technique; **(b)** The photograph of the electrolysis cell for DMES measurement.

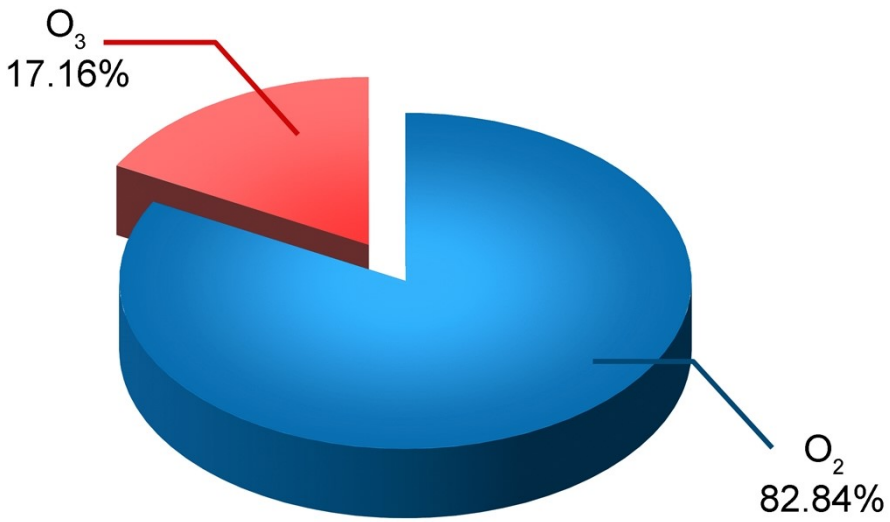

Fig. S30. The quantitative analysis of O_2 and O_3 by DEMS.

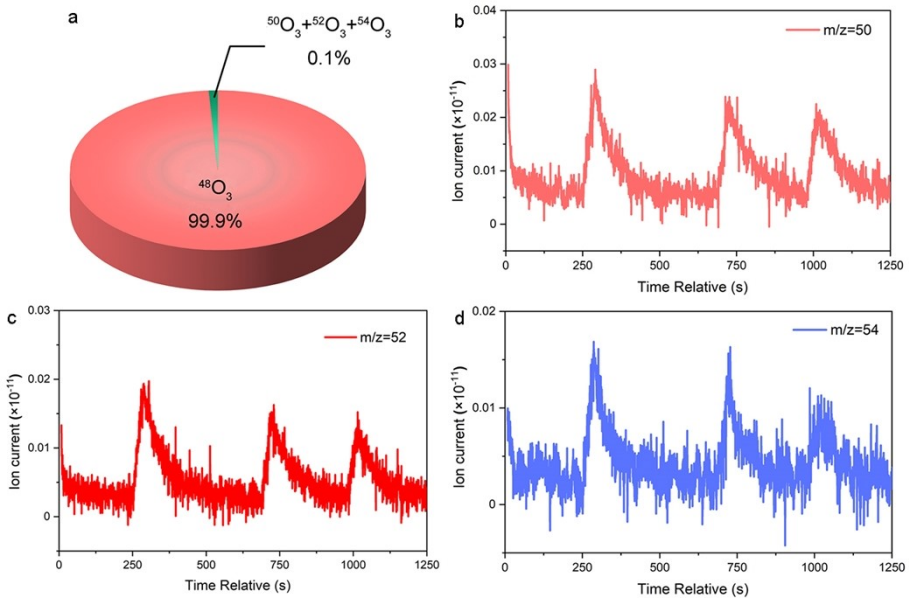

Fig. S31. (a) The mass spectrometry measurements result of O_3; **(b-d)** Differential electrochemical mass spectrometry measurements of m/z=50 ($^{16}O^{18}O^{16}O$), m/z=52 ($^{18}O^{18}O^{16}O$), m/z=54 ($^{18}O^{18}O^{18}O$).

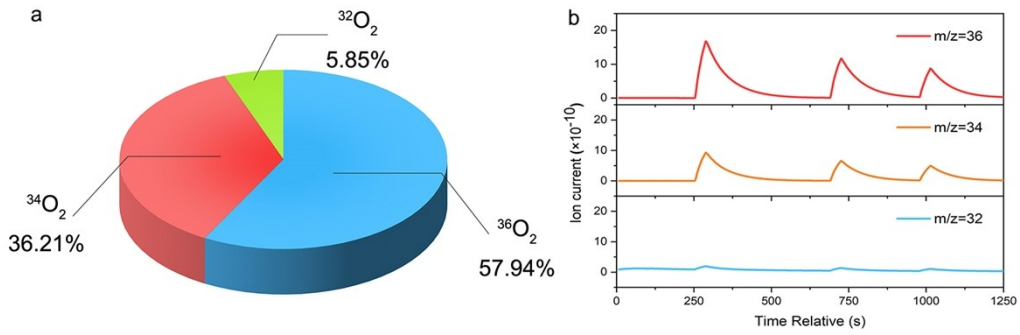

Fig. S32. (a) The Mass spectrometry measurements result of O_2; **(b)** Differential electrochemical mass spectrometry measurements of m/z=36 ($^{18}O^{18}O$), m/z=34 ($^{18}O^{16}O$), m/z=32 ($^{16}O^{16}O$).

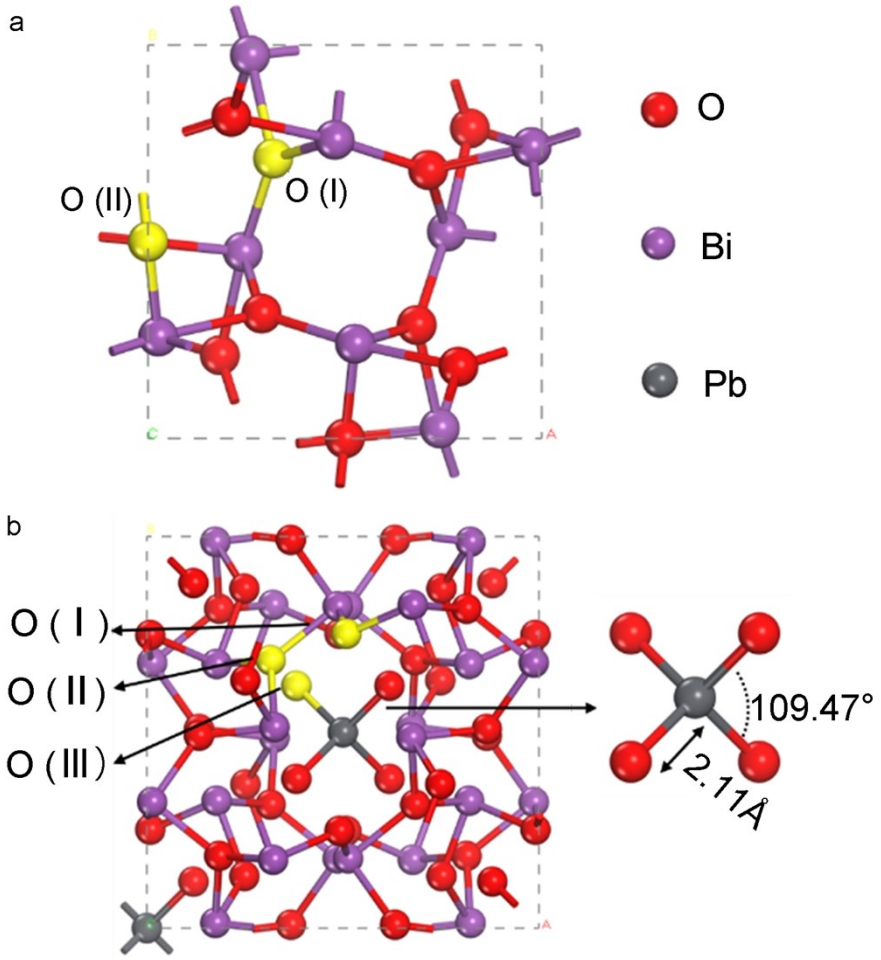

Fig. S33. (a) Bulk structure of Bi_2O_3; **(b)** Bulk structure of $Bi_{12}PbO_{20}$. The purple spheres represent Bi atoms, the gray spheres represent Pb atoms, the red spheres represent O atoms, and the yellow spheres represent O atoms to make the model more intuitive.

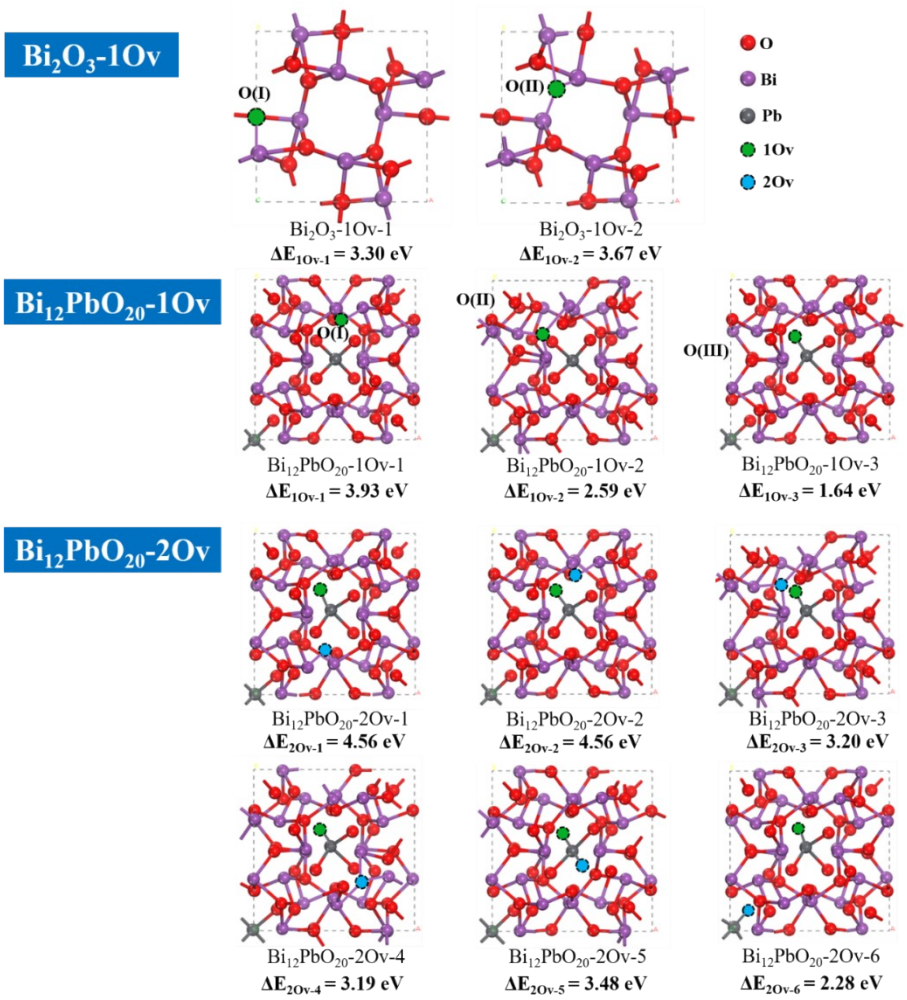

Fig. S34. The optimized structure as well as the corresponding energies with different oxygen vacancy sites.

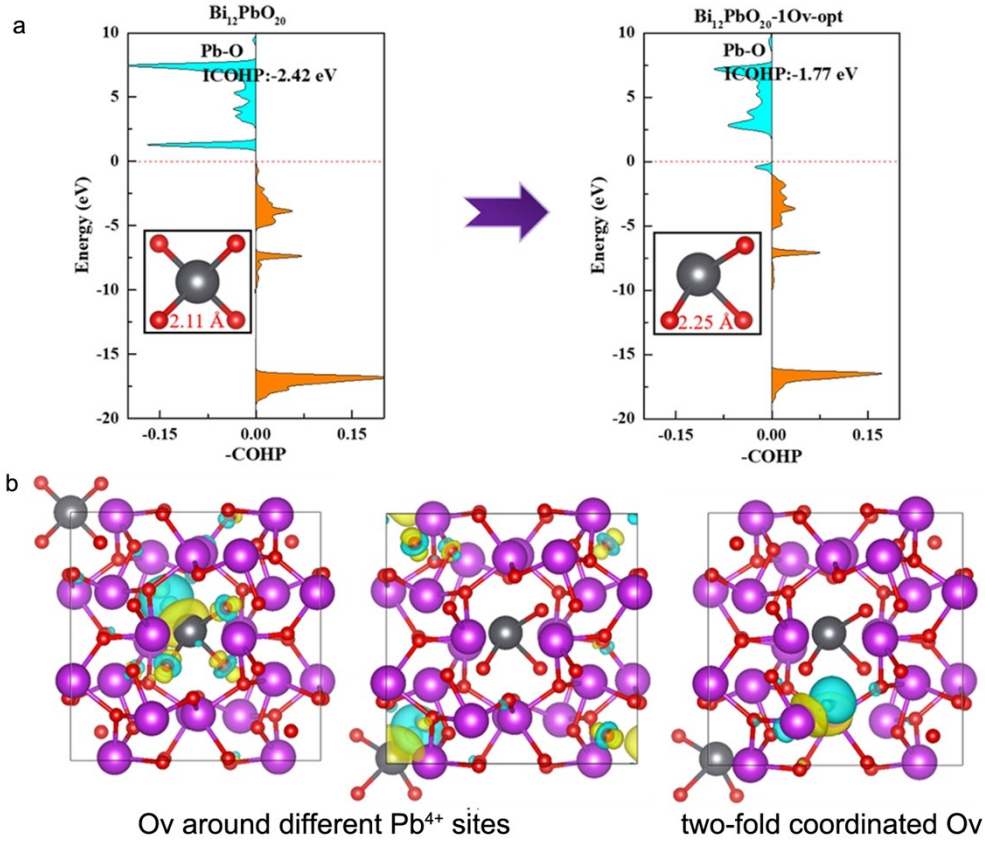

Fig. S35. **(a)** COHP analysis of $Bi_{12}PbO_{20}$ and $Bi_{12}PbO_{20}$-1Ov-opt; **(b)** Calculated charge density differences for $Bi_{12}PbO_{20}$ bulk with different oxygen vacancy sites.

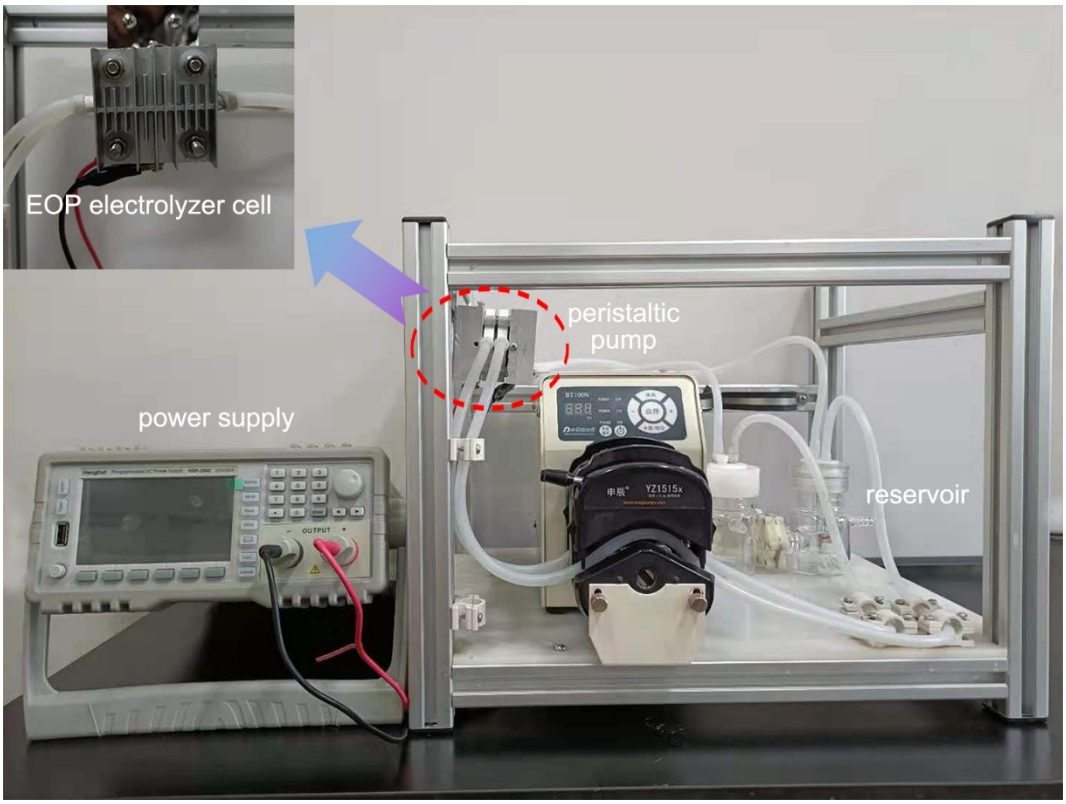

Fig. S36. Photograph of the electrochemical degradation system.